

# Towards Ubiquitous 3D Sensing: Chip-Scale Swept-Source Optical Coherence Tomography

Michael S. Eggleston, Flavio Pardo, Cristian Bolle, Bob Farah, Nicolas Fontaine, Hugo Safar, Mark Cappuzzo, Mark P. Earnshaw

*Nokia Bell Labs, 600 Mountain Ave, Murray Hill, NJ 07974, USA  
Michael.eggleston@nokia-bell-labs.com*

**Abstract:** *Chip-scale OCT has the potential to enable non-invasive and continuous sensing of our surrounding environment and internal physiology. We report our recent work building a swept-source system with >90dB sensitivity at 100kHz using PLC technology.*

**Keywords:** *Photonic Integration, Planar lightwave circuits (PLC)*

## I. INTRODUCTION

Optical coherence tomography (OCT) is a high-speed interferometric-based three-dimensional imaging technique that can provide better than 10 $\mu$ m resolution in all three dimensions. First pioneered for ophthalmology [1], OCT is showing increasing promise not only in other medical fields but also beyond medical applications including in-room LIDAR [2] and non-destructive material analysis [3]. Much of the success of OCT has relied on technological innovations borrowed from the telecom space, including tunable lasers, fiber-based interferometers, and balanced photodetectors. The future of OCT systems – specifically the complete optoelectronic integration to chip-scale for low-cost mass-produced systems – will also borrow heavily from lessons learned in the telecom industry’s drive to produce more complex optical transceivers at lower cost, lower power, and larger volume. Fully integrated, miniaturized OCT systems have the potential to enable a new era of sensing by providing ultra-portable, high-resolution, real-time 3D imaging in any internal physiological or external physical environment.

In this paper, we describe our recent work building towards a fully integrated chip-scale OCT system [4] using a Planar Lightwave Circuit (PLC) interferometer, integrated balanced photo-diodes, and a co-packaged thermally actuated MEMS mirror to achieve a compact and ultra-high sensitivity core optics engine. We achieve a sensitivity >90dB with an optical power of 550 $\mu$ W at the sample in a swept-source OCT system operating at 100kHz.

## II. FIRST GENERATION PLC-BASED INTEGRATED OCT SYSTEM

Recent work on chip-scale, miniaturized OCT has mainly relied on bulky external beam-steering optics and an external interferometer [5], [6] with integrated photonics only providing the optical detection functionality. Previous attempts to use an on-chip interferometer for spectral domain OCT were limited in sensitivity to -53dB due to high losses getting on and off-chip and large backscatter noise in high index contrast silicon waveguides [6]. Chip-scale time-domain OCT has achieved higher sensitivity of -93dB [7] but at the expense of a significantly slower A-scan rate (<2kHz) which ultimately limits image size and leaves the system highly susceptible to motion artifacts. We have recently demonstrated a swept-source OCT (SS-OCT) system, depicted schematically in Fig.1(a), capable of >90dB sensitivity at A-scan rates of 100kHz. The system is comprised of three main components: 1) a portable scanner “puck” with integrated optics engine, beam scan control, and a transimpedance amplifier (TIA), 2) an off-board commercial swept-source OCT laser (Axsun, 1310nm center wavelength, 140nm sweep bandwidth, 100kHz repetition rate), and 3) a mini-computer with a two channel, 16bit, 1 GSAMPLE/sec analog-to-digital (ADC) converter card. The off-board laser and electronics are coupled to the scanner with a single mode fiber, RF data coaxial cable, and USB cable which provides power and communication with the beam sweep controller.

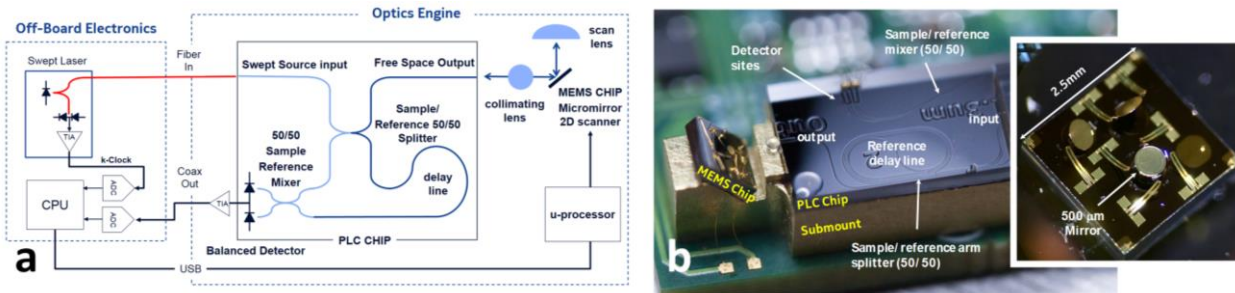


Figure 1. (a) Schematic diagram of the compact OCT system, showing the main components of the Optics Engine and off-board electronics. (b) Partial view of the first-generation OCT Optical Engine. (inset) Detail of the original MEMS mirror and 4 thermal actuators capable of  $\pm 13^\circ$  mechanical tilt.

Fig.1(b) shows an image of the Optical Engine illustrated schematically in Fig.1(a). It consists of a PLC interferometer with integrated photodetectors (PD), coupled to a MEMS 2D scanning mirror by a ball lens, all mounted on a 20mm x 6mm CNC-machined metal submount, which is glued to a rounded 3.5cm x 3.5cm PCB with active components wire-bonded to the detection and driving electronics. The entire PCB is mounted in a 3D printed plastic puck measuring 5cm in diameter and 2cm thick. The top of the puck is closed with a 3D printed lid containing a 4mm focal length scan lens that is aligned directly over the MEMS mirror.

The scanning micromirror consists of a polysilicon 500  $\mu\text{m}$  diameter mirror with a radius of curvature of 100 mm and is driven by four thermal actuators. A soft, serpentine spring connects the mirror with each of the actuators. Each actuator is made of a stack of polysilicon and metal generating a stress gradient across its thickness that bends upwards upon release [8]. Joule heating combined with the differential thermal expansion coefficients between the two materials in the stack flatten each actuator towards the substrate at about 40mW. By suitable combination of the electrical power dissipated in each actuator, piston ( $\sim 200\mu\text{m}$  displacement) and tip tilt motion ( $\pm 25^\circ$  mechanical) can be obtained in our driving system. The thermal time constant for these actuators is  $\sim 3\text{ms}$ , with underdamped characteristics, with a higher frequency mechanical resonance at  $\sim 1\text{kHz}$  ( $Q$  of  $\sim 10$ ) for the mirror-supporting springs system. A two-step driving scheme [9] was easily implemented in the microprocessor to suppress the characteristic ring-down time of more than 10ms.

The CNC-machined metal submount provides a rough mechanical positioning (not better than 50  $\mu\text{m}$ ) for the PLC and MEMS chips, so that the output waveguide is aligned to the center of the MEMS mirror at  $45^\circ$ . Next, a laser source is connected to the PLC and a 500 $\mu\text{m}$  glass ball lens, AR-coated for 1300nm wavelength range, is placed between the two and moved until a narrow, collimated beam is obtained at the imaging plane. A drop of UV-curable cement at the machined pedestal right below the lens location fixes it in place. Although done manually in this work, the entire assembly process, including lens pick-up, active optical alignment, epoxy dispense and curing, can be automated using a programmed stage system [10].

The analog OCT signal from the TIA is fed through a coaxial cable to an external computer, digitized and then processed with an Intel i7 CPU. The signal is resampled using the swept-laser's k-clock and converted to distance using an FFT. Two A-scans (axial scans) are averaged to create a single depth scan and the laser spot is scanned over an area of 1.3mm x 1.3mm. Resultant 3D images of a fingertip are shown in Fig.2(b). A neutral density filter and silver mirror was used to measure a system sensitivity of -90dB.



Figure 2. (a) OCT head. PCB board with mounted optical engine. (b) Two views of the in-vivo 3D rendered OCT data of approximately  $1.3 \times 1.3 \times 1.5\text{mm}^3$  region of a fingertip.

### III. TOWARDS A FULLY INTEGRATED OCT SYSTEM

While our previous demonstration showed a fully integrated optics engine comprised of the OCT interferometer and beam steering elements, it still relied on an external laser and mini-PC. Electronics integration is fairly straight-forward, as an FPGA or ASIC can easily take the place of the external PC. Commercial swept-source lasers are typically

packaged in a compact 14-pin butterfly package but rely on external electronics and fiber-based k-clocks for sweep control and diagnostics which significantly increase overall laser module size and power consumption. The fiber k-clock, which physically consists of an asymmetric interferometer, is very similar to the main OCT interferometer but contains a known interferometer path length delay. The k-clock can then be integrated in the PLC platform as well, with another integrated delay line to set a stable pathlength offset. Our next generation optical engine, as shown in Fig. 3(b), consists of a two channel PLC chip that contains both the initial OCT interferometer and the k-clock interferometer. A waveguide coupler is used to separate approximately 3% of the input laser signal for the k-clock function with the remaining 97% used for the OCT signal. The output of the k-clock interferometer is fed into a balanced diode pair, amplified, digitized and finally the instantaneous phase is calculated using a simple Hilbert transform. The unwrapped k-clock phase is then used as the interpolation spacing to resample the OCT signal. Fig. 3(b) plots the fourier-transformed resampled k-clock from our PLC interferometer, showing the very high signal-to-noise ratio (>60dB) achieved in this simple system. Cross-talk between the OCT and k-clock channels was measured to be >50dB, limited by the cross-talk of the ADC chip used.

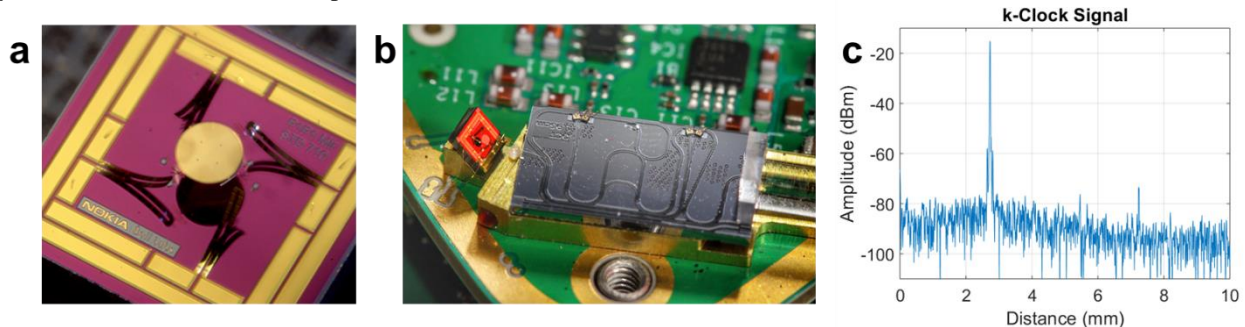


Figure 3. (a) Second-generation thermally actuated MEMS mirror capable of  $\pm 25^\circ$  mechanical tilt angles. (b) PLC chip with integrated OCT interferometer and k-clock interferometer. (c) Single A-scan acquisition from the k-clock channel showing >60dB signal to noise ratio.

#### IV. CONCLUSIONS

We have demonstrated the first chip-scale SS-OCT optical engine with integrated interferometer, laser k-clock, and micro-scanning mirror. The ultra-low loss PLC platform enables a sensitivity of -90dB, high SNR k-clock, and the integrated thermally actuated MEMS provide scan angles up to  $\pm 25^\circ$  mechanical. Such a high-sensitivity chip-scale system is a key component of future fully integrated OCT systems for low-cost and ubiquitous 3D imaging.

#### REFERENCES

- [1] M. Adhi and J. S. Duker, "Optical coherence tomography – current and future applications:," *Curr. Opin. Ophthalmol.*, vol. 24, no. 3, pp. 213–221, May 2013.
- [2] Z. Wang *et al.*, "Cubic meter volume optical coherence tomography," *Optica*, vol. 3, no. 12, p. 1496, Dec. 2016.
- [3] D. Stifter, "Beyond biomedicine: a review of alternative applications and developments for optical coherence tomography," *Appl. Phys. B*, vol. 88, no. 3, pp. 337–357, Aug. 2007.
- [4] M. S. Eggleston *et al.*, "90dB Sensitivity in a Chip-Scale Swept-Source Optical Coherence Tomography System," in *Conference on Lasers and Electro-Optics*, 2018, p. JTh5C.8.
- [5] Z. Wang *et al.*, "Silicon photonic integrated circuit swept-source optical coherence tomography receiver with dual polarization, dual balanced, in-phase and quadrature detection," *Biomed. Opt. Express*, vol. 6, no. 7, p. 2562, Jul. 2015.
- [6] S. Schneider, M. Lauermaun, P.-I. Dietrich, C. Weimann, W. Freude, and C. Koos, "Optical coherence tomography system mass-producible on a silicon photonic chip," *Opt. Express*, vol. 24, no. 2, p. 1573, Jan. 2016.
- [7] J. Sancho-Durá, K. Zinoviev, J. Lloret-Soler, J. L. Rubio-Guviernau, E. Margallo-Balbás, and W. Drexler, "Handheld multi-modal imaging for point-of-care skin diagnosis based on a kinetic integrated optics optical coherence tomography," *J. Biophotonics*, p. e201800193, Jul. 2018.
- [8] J. Morrison, M. Imboden, T. D. C. Little, and D. J. Bishop, "Electrothermally actuated tip-tilt-piston micromirror with integrated varifocal capability," *Opt. Express*, vol. 23, no. 7, p. 9555, Apr. 2015.
- [9] "High-Speed Control of Electromechanical Transduction: Advanced Drive Techniques for Optimized Step-and-Settle Response of MEMS Micromirrors," *IEEE Control Syst.*, vol. 36, no. 5, pp. 48–76, Oct. 2016.
- [10] Y. Gao *et al.*, "Hybrid Integration With Efficient Ball Lens-Based Optical Coupling for Compact WDM Transmitters," *IEEE Photonics Technol. Lett.*, vol. 28, no. 22, pp. 2549–2552, Nov. 2016.